Advanced Herbal Medicine, Summer and Autumn 2021; 6(2): 49-74

herbmed.skums.ac.ir

Berberis vulgaris extract-based Fe_3O_4 nanocomposites affect NMDA1 function and physical activity: *Analysis of Grin1* expression in Syrian mice model of Experimental autoimmune encephalomyelitis

Fatemeh Noruzifard[1], Amaneh Javid[1*], Seyed Mohsen Miresmaeili[1]

[1] Department of Biology, Faculty of Science and Engineering, Science and Arts University, Yazd, Iran.

Received: 05 June 2021 Accepted: 15 September 2021

Original Article

Abstract:

Background: Ionotropic glutamate NMDA receptors are multi-subunit proteins with few selective pharmacological ligands and are tentatively implicated in MS and other neurodegenerative disorders. The present study was aimed at evaluating the antioxidant properties of *Berberis vulgaris* extract-loaded magnetite nanoparticles on the *Grin1* gene expression in NMDA receptor in EAE Syrian mice.

Methods: EAE mice models were generated through active immunization with MBP and PTx and kept for days 9-14 until EAE signs appeared followed by administration of barberry extract loaded magnetic nanoparticles.

Results: Pure BE concentrations did not show recovery signs until days 7-9, but partial recovery in tail movement was seen on days 11 and 14, which was significant as compared to the control group in terms of improvement of the clinical scores. Meanwhile bare nanoparticles had neither disease recovery/progression properties nor EAE mice mortality as compared to controls, but 1 mg BE + Fe_3O_4 reduced EAE symptom severity and resulted in significant improvement of hind limb sensitivity to toe pinching and improved tail movements. Meanwhile 2 mg Be + Fe_3O_4 showed much better sensitivity to toe pinching and complete tail recovery. qRT-PCR analysis showed a significant decrease in relative *Grin1* expression in female mice after treatment with 0.2 and 1 mg BE. However, a profound decrease in *Grin1* expression was seen at 0.2, 1 and 2 mg BE + Fe_3O_4 treated groups in a dose-dependent manner.

* Corresponding author: Department of Biology, Faculty of Science and Engineering, Science and Arts University, an. Tel: 098-3538264080. E-mail address: a_javid@ut.ac.ir

Conclusion: The results indicated that Fe_3O_4+ BE could alleviate the EAE severity and progression

Keywords: NMDA, Neuroprotection, *Grin1*, Syrian mice, *Berberis* vulgaris

INTRODUCTION

N-methyl-*d*-aspartate receptors (NMDARs) are ionotropic glutamate receptors, vital for mediating ion-flux, controlling synaptic plasticity, memory function and cell signaling. Glutamate NMDA-receptor subunit zeta-1 is a protein that is encoded by *GRIN1* gene in humans. NMDARs exist as multiple subtypes, are spatially and developmentally regulated, and are differentially distributed across neuronal subtypes (1). This complex diversity, coupled with a subtype-dependent permeability to calcium influx, makes NMDARs the predominant molecular devices for controlling complex experience-dependent spine remodeling and long-lasting synaptic changes. Such enduring changes in synaptic strength are crucial for associative learning, working memory, behavioral flexibility, or attention (2, 3).

Of the eight subunits, identified as NMDA receptor components, a minimal configuration in heterologous expression of the NMDA receptor appears to be two pairs of GLUN1 and GLUN2 subunits, although it appears more likely that, physiologically, NMDA receptors are mixtures of all three subunit groups (GLUN1, GLUN2, and GLUN3, encoded by the genes *GRIN1*, *GRIN2A/2B/2C/2D*, and *GRIN3A/3B*) (4, 5). NMDA receptors open to allow a large influx of calcium, but only after the receptor's cell has been depolarized repeatedly over a period of hundreds of milliseconds (6-8). This calcium influx modulates various cellular mechanisms by activating Ca^{2+}/calmodulin-dependent kinases, protein kinase C (PKC), phospholipase C (PLC)/A2, calcineurin, and nitric oxide synthase (9). In cases of strong, prolonged NMDA stimuli, this calcium signaling is huge enough to damage the cell and can even be fatal. Functionally, the duration and amplitude of the NMDA response is modulated by various ions, endogenous molecules and psychotropic drugs (10).

The barberry fruit is a well-known ingredient in Iranian cuisine (11, 12). The root, bark, leaf and fruits of barberry are used in the Traditional Persian Medicine (TPM) as immune-modulators, anti-microbial agents, and in the treatments for the central nervous system and cardiovascular, gastrointestinal, endocrine, and renal

disorders (13). It has been observed in recent studies that barberry and berberine (barberry's main phytochemical) have antioxidant, anti-inflammatory, antitumor, antimutagenic, antidiabetic, neuroprotective, and hepatoprotective effects. *Berberis vulgaris* may play preventive role in morphine-consumption relapse in addicted individuals (14). Low solubility is the most important limitation of herbal extracts (15), while magnetic nanoparticles can prove to be appropriate carriers with good superparamagnetic properties and could carry high amounts of important phytochemicals and deliver them to different cancer tissues. The barberry extract (BE)-loaded Fe_3O_4 nanoparticles could destabilize endo/lysosomal membranes and improve the natural compounds' release to the cytosol (16).

Given the neuroprotective and antioxidant roles of *B. vulgaris*, the aim of the present study was to evaluate, for the first time, the antioxidant properties of *Berberis vulgaris* extract-loaded magnetite nanoparticles on the physical symptoms of MS and the *Grin1* gene expression in the NMDA receptors in the prefrontal cortex region of EAE mice brain tissues.

MATERIALS AND METHODS

Barberry fruit extraction and qualitative phytochemical-detection

For hydroalcoholic extraction of B. vulgaris fruits, Soxhlet extraction method (17) with 30% water was used: 70% ethanol as solvent. First, impurities were removed from the fruits and 20 g of dry matter (Dry matter : solvent ratio = 1:10, respectively) was run in Soxhlet apparatus for 5 h. the resultant liquid was filtered and placed in water bath for solvent evaporation. The resultant hydroalcoholic extracts were assessed for the presence of the phytochemical compounds using the following standard methods:

Anthraquinones analysis

10 ml of benzene was added to 6 g BE sample in a conical flask and soaked for 10 minutes and then filtered. Furthermore, 10 ml of 10% ammonia solution was added to the filtrate and shaken vigorously for 30 seconds until pink, violet, or red color indicated the

presence of anthraquinones in the ammonia phase (17).

***Tannin* analysis**

10 ml of bromine water was added to the 0.5 g BE. Decoloration of bromine water showed the presence of tannins (18).

Saponin analysis

5.0 ml of distilled water was mixed with aqueous crude BE in a test tube and mixed vigorously. A few drops of olive oil were added to the froth and mixed vigorously. The foam appearance showed the presence of saponins (19).

Total phenolic content

Total phenolic content was determined using Folin-Ciocalteu (FC) reagent. The plant extract (0.5 mL) was mixed with 0.5 mL of FC (1:1 diluted with distilled water) and incubated for 5 min at 22 °C, followed by the addition of 2 mL of 20% Na_2CO_3. The mixture was then incubated further at 22 °C for 90 min and the absorbance was measured at 650 nm. The total phenolic content (mg/mL) was calculated using gallic acid as standard (20).

Total flavonoid content

The total flavonoid content (mg/mL) was determined using aluminum chloride ($AlCl_3$) method. The assay mixture consisting of 0.5 mL of the plant extract, 0.5 mL distilled water, and 0.3 mL of 5% NaNO2 was incubated for 5 min at 25 °C, immediately followed by addition of 0.3 mL of 10% $AlCl_3$. Two milliliters of 1 M NaOH was then added to the reaction mixture, and the absorbance was read at 510 nm. Quercetin was used as a standard (21).

Glycoside analysis

Liebermann's Test: 2.0 ml of acetic acid and 2 ml of chloroform were mixed into whole aqueous BE. The mixture was then cooled and mixed with H_2SO_4 (conc.). Appearance of green color showed the steroidal components of glycosides (22).

Keller-Kiliani Test: Glacial acetic acid solution (4.0 ml) and 1 drop of 2.0% $FeCl_3$ mixture was mixed with the 10 ml aqueous BE and 1 ml H_2SO_4 (conc.). Formation of brown ring between the layers showed the cardiac steroid component of glycosides.

Salkowski's Test: 2 ml H2SO4 (conc.) was added to the whole aqueous BE. Formation of reddish brown color indicated the presence of steroidal aglycone component of glycosides.

Terpenoid analysis

2.0 ml of chloroform was added to 5 ml aqueous BE and evaporated on the water bath. The mixture was then boiled with 3 ml of H_2SO_4 (conc.). Formation of grey color showed the terpenoids (17-20).

Steroid analysis

Two ml of chloroform and H_2SO_4 (conc.) were added with the 5 ml aqueous BE. Formation of red color in the lower chloroform layer indicated the presence of steroids (23).

Alkaloid analysis by Wagner test:

Two ml BE filtrate was mixed with 1% HCl and steamed. Twelve drops of Wagner reagent were added to the resultant solution. Appearance of brownish-red precipitate indicated the presence of alkaloids (23).

Fe_3O_4 nanoparticle synthesis and BE loading

Bare Fe_3O_4 nanoparticles (NPs) were prepared by chemical co-precipitation technique, with some modification in the previously described method (24, 25). Briefly, 5.41 g of $FeCl_3 \cdot 6H_2O$ (99% purity) and 1.99 g $FeCl_2 \cdot 4H_2O$ (99% purity) were dissolved in 100 ml of distilled water (DW) in a triple-necked flask. The pH of the mixture (100 ml) was maintained at pH 6.9 through the slow addition of 25 ml of NH4OH (25–28%, w/w) while stirring constantly under the protection of dry nitrogen at 60 °C. At this time, the solution color changed from yellow to deep black, indicating the formation of Fe_3O_4 particles. After 1 h of stirring, Fe_3O_4 NPs were rinsed with DW and subsequently incubated with BE overnight at 37 oC. The resultant product was then sonicated for 1h, centrifuged at 10,000 rpm for 30 min. and vigorously stirred for 1 h at 45 °C under nitrogen atmosphere. The resulting nano-biocomposites were stored at 4 °C till further use.

Study design and Ethical Considerations

This study was carried out at the Central Biology Lab of Faculty of Science and Engineering, Science and Arts University, Yazd, Iran, and was approved by the Ethics Committee of Academic Center for Education, Culture and Research (ACECR), Iran. Animal welfare and ethical considerations were followed as per The Guide for the Care and Use of Laboratory Animals throughout the experiments and the least number of animals were considered for all treatment groups to reach satisfactory statistical significance.

Preparation of MBP emulsion and Pertussian toxin for active immunization

For a 200 µl injection (200 µg myelin basic protein (MBP)) to each mice, 1:1 ratio of MBP solution and CFA were prepared. For this, lyophilized MBP (Becton, Dickinson and Company, Sparks, MD, USA) was diluted in ddH_2O to a final concentration of 2 mg/ml and stored at -20 °C for further use.

For subcutaneous administration in each flank of mice, the stock solution of pertussis toxin was prepared as follows: 4 µg of pertussis toxin (PTx; Sigma Chemicals, St. Louis, MO, USA) was diluted in 2 ml of PBS and stored at 4 °C. For each injection of 200 µl, 400 ng PTx was selected, as described previously (26).

Generation of chronic EAE mice models through active immunization

For generating EAE mice models through active immunization (27), sixteen male and sixteen female Syrian mice (also called mouse-like hamsters - age: 8-12 weeks; weight range: 35.5 ± 1.0 g) were purchased from the Research and Clinical Center for Infertility, Yazd, Iran. Two mice from each sex group (female, n=2; male, n=2) were selected as control group candidates. The animals were housed in standard cages, 4 mice/cage, and maintained under standard experimental conditions (12h light/12h dark cycles; 22 ± 3.5 °C; 50% relative humidity), with free access to food and water. The mice were kept in above-mentioned condition for one week to reach stable physiological condition. For active

immunization, the mice were injected subcutaneously in each flank with 200 μg of MBP/mice at Day 0. Pertussis toxin was injected intraperitoneally (i.p.; 400 ng/mice) at days 1 and 2. A control group of mice received MBP suspension alone.

EAE scoring

Mice were observed daily for clinical scores and body weight. Disease severity and clinical symptoms were scored as follows: 0, normal; 1, loss of tail tone; 2, hind limb weakness; 3, hind limb paralysis; 4, hind limb paralysis and forelimb paralysis or weakness; 5, moribund/death. Onset of chronic illness should happen within days 9-14 while days 12-19 (post-onset) are considered to be peak severity of disease. A small number of animals may exhibit the symptoms of remitting-relapsing type of the disease.

EAE Treatment groups and Brain region dissection

The experiment was carried out in 7 treatment groups and 1 control group (each group, n=4 (2 male, 2 female mice)). The 7 treatment groups comprised three BE groups (0.2, 1 and 2 mg BE), three BE-Fe_3O_4 groups (0.2 mg BE+ Fe_3O_4; 1 mg BE+ Fe_3O_4 and 2 mg BE+ Fe_3O_4) and one bare Fe_3O_4 nanoparticle group. Mice were anesthetized with ketamine and xylazine (i.p., 100 and 50 mg/kg, respectively) and were promptly euthanized. The animals were decapitated, and the brain regions were dissected accordingly to "The Rat Brain Stereotaxic Coordinates". Both sides of the prefrontal cortex (PFC) were collected and left in a freezer at 20 °C for further analysis.

RNA isolation and cDNA synthesis

Total RNA from dissected PFCs was isolated with RNeasy Mini Kit (Qiagen). Quality and integrity of the samples were verified after the RNA isolation using NanoDrop UV-Vis. Spectrophotometer (ScanDrop^2, AnalytikJena, Germany) using butterfly cuvettes and electrophoresed (2% agarose gel), respectively. Only samples with satisfactory quality and without degradation or impurities were used in this study. The reverse transcription reaction was performed using RevertAid™ cDNA Synthesis kit (Cat. No. K1621; Thermo Fisher Scientific

Inc. Waltham, Massachusetts, USA), according to the manufacturer's instructions.

Grin1 expression analysis by RT-PCR

Grin1 TaqMans probe was used to evaluate the expression of glutamatergic NMDAR. *Grin1* expression was analyzed using SYBR Green as fluorophore. For this purpose, *GAPDH* was used as endogenous control. *GAPDH* (20 bp) and *Grin1* (20 bp) primer sequences were as follows, respectively:

GAPDH	F: CTCATTTCCTGGTATGAGAG
GAPDH	R: TCAACCTTCGCTCGTCTGCT
Grin1	F: ACTCCCAACGACCACTTCAC
Grin1	R: GTAGACGCGCATCATCTCAA

All reactions were performed in triplicates in the qTOWER2.2 Quantitative Real-Time PCR (Thermal Cycler, Analytik Jena, Germany), according to cycling conditions, recommended by the manufacturer. For the relative quantification, we used the comparative Ct method, and $2^{-\Delta CT}$ values (ΔCt¼target gene Ct − endogenous gene Ct) were used for the statistical analysis.

Statistical Analysis

Data were presented as mean ± SD using SPSS (version 16). The data were analyzed by one-way ANOVA. Significance level was considered $p \leq 0.05$. Normality (Shapiro-Wilk) and homogeneity (Levene's) tests were performed using $2^{-\Delta CT}$ as dependent variable for the experimental design. Student's t-test was performed to compare treatment and control groups.

RESULTS

Quantitative analysis of BE phytochemicals

Hydroalcoholic extraction of *B. vulgaris* fruits was carried out using Soxhlet extraction and the qualitative analysis of its key phytochemicals was performed accordingly. Present results indicate that the BE contained anthraquinones, tanins, saponins, phenols, flavonoids, glycosides, triterpenoids, steroids and alkaloid content, which indicates the antioxidant rich composition of BE (Table 1).

Table 1. Qualitative analysis of BE phytochemicals.

Phytochemical Type	Phytochemical Test (+/-)	Phytochemical Type	Phytochemical Test (+/-)
Anthraquinones	+	Tanins	+
Saponins	+	Total phenols	+
Total flavonoids	+	Glycosides	+*
Triterpenoids	+	Steroids	+
Alkaloids	+	*Both qualitative tests of glycosides showed positive results.*	

Abbreviation: BE = *Berberis vulgaris* extract.

Table 2. SEM, zeta potential and size distribution analysis results for bare and BE-loaded nanocomposites.

Particle type	SEM morphology	DLS analysis			
		ζ Potential (mV)	Size distribution (nm)	Temp. (^{o}C)	pH
Fe_3O_4	Partially Globular forms with dense structures	-42±2.5	79±4.8	25	7.0
BE-Fe_3O_4	Globular and non-agglomerated forms	-11±8.9	182±3.9	25	7.0

Abbreviations: BE = *Berberis vulgaris* extract; SEM= Scanning Electron Microscopy; DLS= Dynamic Light Scattering; ζ Potential= Zeta potential; Temp.= Temperature.

Magnetite nanoparticle synthesis and characterization

Magnetite (Fe_3O_4) nanoparticles were synthesized by chemical co-precipitation technique and their chemical and physical characterization was done as follows:

Electron microscopy and Dynamic Light Scattering analysis

TEM micrographs revealed interesting results about the bare (Figure 1A) and BE-loaded Fe_3O_4 (Figure 1B) nanocomposites. Bare Fe_3O_4 nanoparticles were less globular entities, agglomerated together, while having <100 nm average size, but BE-loaded nanocomposites were true spherical forms with much less agglomeration characteristics, while having larger average diameters.

The nanocomposite samples were then analyzed with Dynamic Light Scattering (DLS) technique to assess zeta potential and average diameter at 25 ^oC and pH=7.0. Figure 1 indicates particle size distribution and hydrodynamic diameter histograms of bare (C) and BE-loaded (D) Fe_3O_4 nanocomposites, which were 79±4.8 and 182±3.9 nm in diameter, respectively. The bare nanoparticles had a negative zeta potential (-42±2.5 mV), which is the result of formation of Fe-OH_{aq} linkages, while in BE-loaded nanocomposites, the zeta potential reached a high positive number (-11±8.9 mV) (Table 2).

Fourier-transform infrared spectroscopy (FTIR)

FTIR analysis can clearly reveal the presence and type of bonds/interactions that may occur between two or more entities in a complex. Figure 2 shows FTIR spectra of bare and BE-loaded Fe_3O_4 nanocomposites. According to our results, Figure 2 (A) shows the BE spectrum, according to which 702.51, 901.01 and 1315.34 cm^{-1} peaks were related to the C-C, carbon (weak peak) and C-H stretching vibrations, while the peak of 3865.90 cm^{-1} indicates flavonoid-OH stretching vibrations in BE. According to Figure 2 (B), the Fe_3O_4 spectrum revealed Fe-O stretching vibrations at 687.01 cm^{-1}, which shows a clear shift at 671.19 cm^{-1} in the BE-Fe_3O_4 spectrum, indicating nanoparticle-BE interaction. In addition,

1090.25, 1354 and 1635.54 cm^{-1} peaks in BE-Fe_3O_4 spectrum indicate the stretching vibrations of C-O, C-H and C≡C. Peak at 2710.45 cm^{-1} shows the C-H stretching vibrations in saponins and alkaloids. Besides that, 3440.10 and 3195.92 cm^{-1} demonstrate the O-H stretching vibrations in Fe_3O_4 nanoparticles and the shift in this region, respectively. The FTIR analysis clearly shows the interactions between BE and nanoparticles.

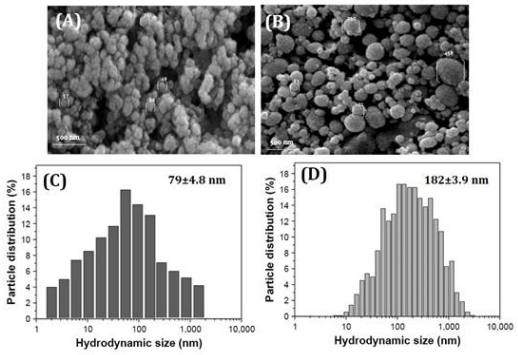

Figure 1. SEM micrographs of (A) bare and (B) BE-Fe_3O_4 NPs. Size distribution and hydrodynamic diameter (C) bare and (D) BE-Fe_3O_4 NPs by DLS at 25 °C and pH=7.0.

EAE induction in Syrian mice

EAE induction in Syrian mice showed promising results and the mice started showing disease symptoms 14 days post-injection of MBP and PTx. According to Table 3, both male and female mice showed slight alteration in body weight and various physical symptoms, ranging from tail limps to tail and hind limb paralysis, which was clearly evident on days 5-14 post-injection. The limb paralysis caused the animals to show no response to toe stimulation and pinching.

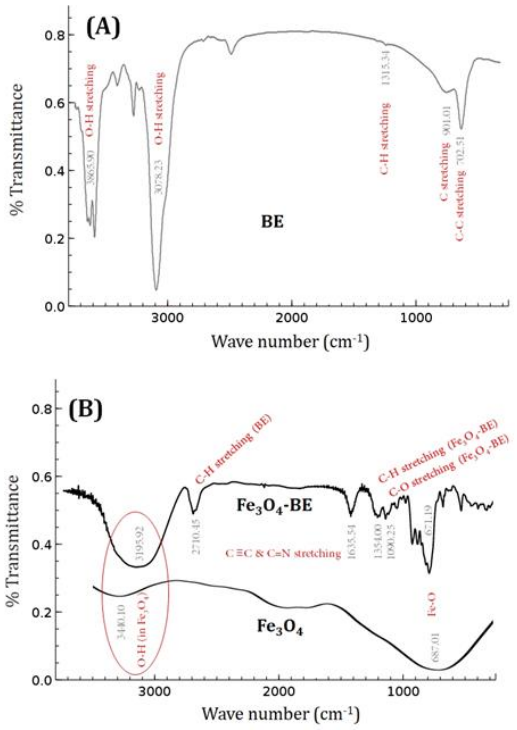

Figure 2. FTIR spectra of (A) pure BE and; (B) comparison spectra for Bare Fe_3O_4 and BE-Fe_3O_4.

Symptoms progressed in a predictable manner and most of the EAE mice displayed motor deficits, tail limp and partial fore or hind limb paralysis (Table 3 and Figure 3A-C). Disease symptom monitoring was

carried out after almost every alternate day. Male mice showed a slight increase in body weight during the disease induction period of 14 days, while female mice did not show significant weight gain (Table 3).

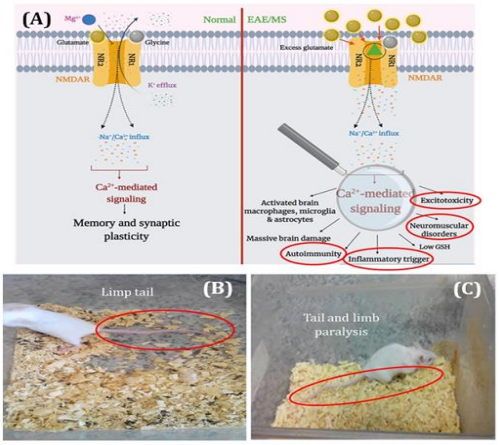

Figure 3. (A) Limp tail and (B) limb and tail paralysis in EAE mice. (C) Schematic diagram of key signs and symptoms of MS/EAE disease and the difference in cell metabolism between MS/EAE and normal individuals. The red circles show the signs and symptoms, observed in EAE models of both sexes.

Relation between sex difference and clinical scores in EAE mice

EAE clinical scores for male and female mice, immunized with MBP beforet PTx-injection, (one MBP and two PTx shots) were investigated through 14 days of EAE-induction period. As shown in Figure 4, there was no difference in the extent of disease induction in male and female mice at Day 5 ($p \geq 0.05$) but both sex groups showed the disease symptoms, as illustrated above. On the other hand, the severity of disease symptoms had an aggressive manner (Clinical score ~4) in female mice at Day 7, as compared to the male mice (clinical score ~3; $p < 0.01$) while the prevalence of disease in female mice was more aggressive on day 7, as compared to the male group, which was clearly detectable by partial

hind limb paralysis. On day 11, the mice of both sex groups showed identical symptoms ($P \geq 0.5^{*}$) and there was recorded no difference in peak clinical score (~4). But, the treatment period of 14 days post-injections showed significant severity of EAE score in female mice with paralysis in both limbs and tail (clinical score ~6), as compared to the male mice (clinical score ~4; $p < 0.001$) (Table 3; Figure 4).

Table 3. The body weight and different scoring symptoms in EAE mice models through disease scale 0-10, on day 14 post injection of MBP and PTx

	Day 1	*Day 3*	*Day 5*	*Day 7*	*Day 9*	*Day 11*	*Day 14*
Male mice							
Weight	29.50	29.50	29.58	29.28	29.25	30.1	30.15
Symptoms/Score	Nil/0	Nil/0	Inflated left hind limb/3	Inflated both hind limbs/3	Upper tail limps and Inflated both hind limb/3	Tail and left hind limb paralysis/4	Tail and left hind limb paralysis/4
Female mice							
Weight	27.20	29.10	28.99	28.12	28.13	27.89	27.23
Symptoms/Score	Nil/0	Nil/0	Hind limb inflammation/ 3	Partial paralysis in right hind limb/4	Right hind limb paralysis/4	Right hind limb and tail paralysis/4	Left and right hind limb, and tail paralysis/6

Abbreviations: EAE = Experimental autoimmune encephalomyelitis; MBP = Myelin basic protein; PTx = Pertussian toxin.

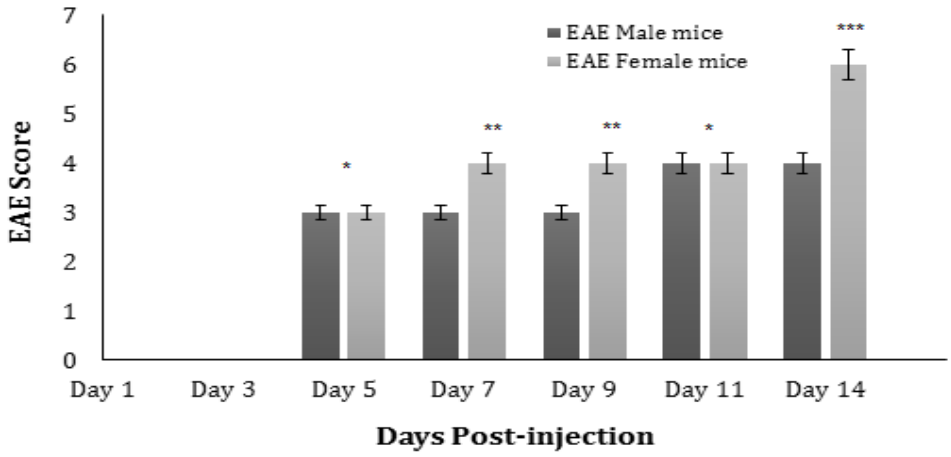

Figure 4. Comparative analysis of EAE symptoms' induction in male and female mice. Both male and female Syrian mice exhibited 100% EAE clinical disease incidence with no mortality. Clinical EAE scores are represented as Mean±SEM. The asterisks show the significance of difference as $^{*}p<0.5$; $^{**}p<0.01$ and $^{***}p<0.001$ between male and female mice, respectively

Fe_3O_4-BE alleviates EAE progression

Two weeks after disease induction and symptom monitoring, we investigated the effect of different concentrations of pure BE at 0.2, 1 and 2 mg BE/kg/dose and the same amounts were loaded onto Fe_3O_4 nanoparticles (fixed concentration for all treatment groups; 0.5 mg/ml) by subcutaneous injection. Our results showed that 0.2, 1 and 2 mg concentrations of pure BE extracts did not show recovery signs until days 7-9. Moreover, partial recovery in tail movement was seen on Days 11 and 14 in both sex groups, which was significant as compared to the control group in terms of improvement in the clinical scores ($p<0.5$).

Meanwhile, bare nanoparticles (0.5 mg/ml) had neither disease recovery/progression properties nor EAE mice mortality ($p\geq0.05$; as compared to control group). Fe_3O_4+ 1 mg BE reduced EAE symptom severity and resulted a significant improvement in hind limb sensitivity to toe pinching and improved tail movements ($p< 0.01$). Meanwhile, Fe_3O_4+ 2 mg BE showed the most significant improvement in EAE recovery and disease scores. The subjects of this group showed much better sensitivity to toe pinching and complete tail recovery ($p< 0.001$) (Table 2). Thus, the results indicate that Fe_3O_4+ 2 mg BE could alleviate the disease severity and progression of EAE.

Excitotoxicity assessment through detection of *Grin1 gene expression in the NR1 subunit of CNS ion channel, NMDA1* in EAE mice brains

Excitotoxicity and *Grin1* gene expression in the NR1 subunit of CNS ion channel, NMDA1, was assessed through RNA extraction and RT-PCR technique for mice brain-tissue sections.

Table 4. The body weight of male and female mice and EAE recovery on day 14 post-treatment.

Treatment sample	*Day 1*	*Day 3*	*Day 5*	*Day 7*	*Day 9*	*Day 11*	*Day 14*	
0.2 mg BE	27.23	27.20	27.19	27.30	27.70	28.01	27.90	Weight
	No recovery	No recovery	No recovery	No recovery	Improved tail movements	Improved tail movements	Improved tail movements	*Disease recovery*
1 mg BE	33.29	33.33	33.21	33.35	33.37	33.34	33.35	Weight
	No recovery	No recovery	No recovery	No recovery	No recovery	Improved tail movement	Improved tail movement	*Disease recovery*
2 mg BE	33.12	33.25	33.30	33.20	33.45	33.40	33.43	Weight
	No recovery	No recovery	No recovery	No recovery	No recovery	Improved tail movement	Improved tail movement	*Disease recovery*
Fe_3O_4 + 0.2 mg BE	33.20	33.21	33.30	33.30	33.45	33.4	33.45	Weight
	No recovery	No recovery	No recovery	No recovery	No recovery	Improved tail movement	Improved tail movement	*Disease recovery*
Fe_3O_4+ 1 mg BE	34.12	34.0	34.15	34.1	34.24	34.12	33.98	Weight
	No recovery	No recovery	No recovery	No recovery	No recovery	Improved tail movement	Tail recovered + improved hind limb sensitivity	*Disease recovery*
Fe_3O_4 + 2 mg BE	33.30	33.30	33.25	33.31	33.38	33.33	33.38	Weight
	No recovery	No recovery	No recovery	Partial recovery in tail and hind limbs	Partial recovery in tail and hind limbs	Hind limb sensitivity to toe pinching	Tail recovered + improved hind limb sensitivity	*Disease recovery*
Bare Fe_3O_4	26.45	26.0	24.15	25.1	27.24	24.32	25.98	Weight
	No recovery	No recovery	No recovery	No recovery	No recovery	No recovery	No recovery	*Disease recovery*
Control	30.15	30.12	30.14	30.24	30.21	30.45	30.45	Weight

According to our results, 0.2, 1 and 2 mg BE-loaded Fe_3O_4 nanocomposites had been shown to disrupt NMDAR's function through the altered expression of *Grin1*. According to Figure 5, qRT-PCR of the treatment and control group mice brain mRNA showed a significant decrease in relative *Grin1* expression in female mice after treatment with 0.2 and 1 mg dose of BE.

A profound decrease in *Grin1* expression was also observed in the Fe_3O_4+ 0.2 mg BE, Fe_3O_4+ 1 mg BE and Fe_3O_4+ 2 mg BE treated groups in a dose-dependent manner ($p<0.001$). Furthermore, bare Fe_3O_4 nanoparticles caused markedly elevated *Grin1* expression after 14 days of treatment period ($p>0.5$).

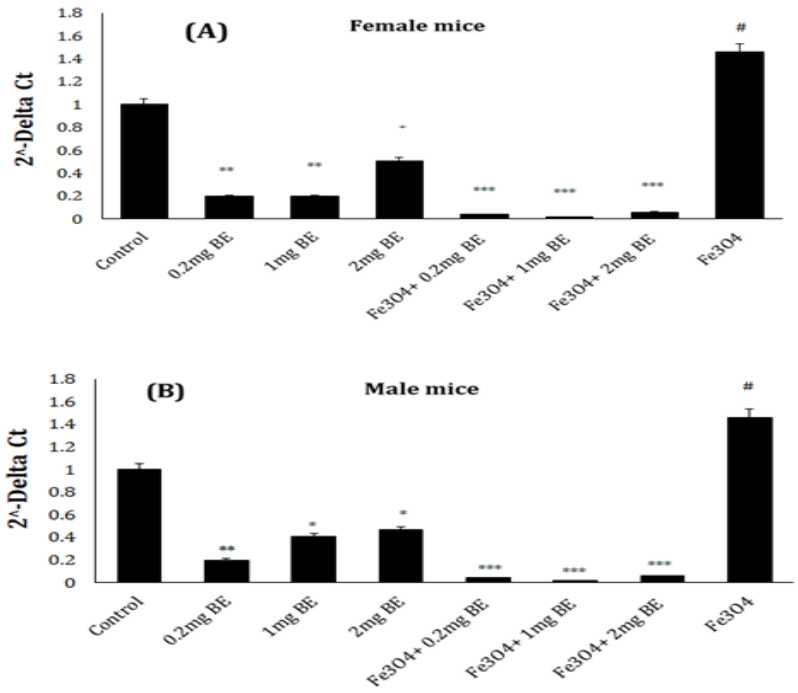

Figure 5. *Grin1* gene expression in control and treatment groups of (A) female and (B) male mice. Data are expressed as Mean±SEM. The asterisks represent the statistical significance of results as: $^{*}p<0.5$; $^{**}p<0.01$; $^{***}p<0.001$ and $^{\#}p\geq0.5$, in comparison to the control group.

Discussion

EAE is a widely accepted model of demyelinating multiple sclerosis (MS) disease. Like MS, EAE is characterized by infiltration of immune cells into the central nervous system (CNS) and demyelination. The two most widely used methods to induce EAE are: active induction by immunization and passive induction through adoptive transfer (26). During this study, EAE mice models were generated through active immunization technique. Active immunization models are the most popular mouse models of multiple sclerosis (MS). Our mice were immunized using neuroantigen, myelin basic protein (MBP), which causes development of activated myelin-specific T cells, trafficking of immune cells into the CNS, and direct damage and inflammation in the CNS. The use of pertussis toxin (PTx) increases both the incidence and severity of disease (26, 28). In our study, the EAE mice model successfully presented MS symptoms, such as ascending paralysis, tail limps and tail and hind limb paralysis, which were readout through *Clinical Score*, and neuroinflammation was evident in the brain tissues of the treatment groups (28). Our results showed that the mice weight loss pattern following EAE progression and pattern of increasing severity in tail and limb paralysis was evident in all EAE subjects during the disease progression period, especially during on days 5-14.

Since the immune system and the immune mechanisms in EAE are very complex, some treatments that have been successful in EAE are yet to be assessed in MS (26, 29). EAE studies may differ widely in terms of the experimental conditions. This includes the species, strain, and sex of the animals used; the age; specific induction method (including the neuroantigen, the type of adjuvant used, the active induction); and the timing, frequency and dose of the therapeutic agent under study (29). Most EAE experiments with rodents are done in genetically identical groups of animals. This at least eliminates an important source of variation (this variation does exist in humans). However, genetically identical animals may differ in susceptibility to EAE depending on environmental factors, which may not be easily controlled. For example, the

degree of gut colonization and the type of commensal flora can largely determine the susceptibility to EAE (30).

Our clinical score analysis across 14 days of EAE induction showed no difference in the extent of disease induction among male and female mice at Day 5. In the meanwhile, both male and female groups exhibited disease symptoms to a varied extent. Our female EAE mice group showed aggressive disease symptoms with clinical score of ~4 on day 7 after disease induction. Furthermore, the male EAE mice showed comparatively milder disease symptoms with clinical score of ~3. Disease prevalence and partial hind limb paralysis was more aggressive in female mice on day 7, as compared to the male group and both male and female mice showed limb paralysis (clinical score ~4) on day 11. Paralysis in both limbs and tail was observed in female mice during the treatment period of 14 days post-injections that is the evidence of substantial severity of EAE score in this group with clinical score of ~6, as compared to the male mice (clinical score ~4). Our sex difference results in EAE induction and progression are in line with the study of Wiedrick et al. (2021). They reported that the sex differences in peripheral immune responses may explain the reduced cellular infiltration and differing chemokine profiles in the central nervous system (CNS) of male and female EAE mice and the reduced CNS infiltration and demyelination observed in male and female EAE groups of mice (31).

MS is more prevalent in women than men (a ratio of 3:1), a phenomenon also seen in several other autoimmune diseases (28-31). So, differences in the immune or nervous system between women and men have been extensively studied, which might be resulted from the effects of hormonal and genetic differences, as well as different factors of environmental exposure and modern lifestyle in men and women (31). Our results showed that the EAE symptoms started with identical extent in the female and male mice, but severity of the disease and symptom scores were significantly higher in female mice as compared to the male group.

MS is an expanding global autoimmune inflammatory disease with complex etiologies. Five main Traditional Persian Medicine (TPM) pharmacopeias from the 9th to the 18th century A.D. have been studied to identify the remedial plants for this disorder. Moreover, PubMed and Scopus databases have been checked to derive relevant activities for these plants. Khaddar (numbness), Esterkha (Palsy) and Falej (quadriplegia) are traditional definitions; clinically relevant to today's "MS disease" (32). Barberry (*Berberis vulgaris*) is a traditional plant that is used in folk medicine and Persian cuisine. It does not have any known toxic side effects at reasonable dosages. Extracts obtained from the roots and fruit of *Berberidaceae* species have been used to boost body's defense system (33). Antineoplastic effects of barberry extract and its key phyto-alkaloid, berberine, have long been proven by various researchers (34). One of the promising ways for the improvement of bioavailability, stability, solubility, and biodistribution of natural products is formulation of these compounds in nanostructured forms (35).

Our previously synthesized superparamagnetic iron oxide nanoparticles (Fe_3O_4) showed good efficacy against ovarian cancer (24). Therefore, barberry extract was loaded onto the Fe_3O_4 nanoparticles in order to evaluate the neuroprotective and anti-inflammatory role of this antioxidant-rich herbal extract on MS. We achieved promising results as our EAE mice showed improvement in limb and tail paralysis, and motor deficits, which was evident after 11th and 14th days of treatment in both male and female subjects. This can be attributed to the antioxidant properties of barberry extract and strong drug delivery and biodistribution properties of our Fe_3O_4 nanoparticles that have already been reported. Recently, numerous studies have been carried out on the application of herbal compounds to improve myelin repair and suppress the inflammation (36).

Our study has shown that *Berberis vulgaris* extract-loaded magnetite nanoparticles could cause partial recovery of tail movement and improvement in clinical scores at days 11 and 14 in both sex groups as

compared to the control group. Furthermore, bare magnetic nanoparticles neither showed disease recovery/progression functionality nor EAE mice mortality. Meanwhile, Fe_3O_4 + BE showed the most significant improvement in EAE recovery and disease scores and better sensitivity to toe pinching and complete tail recovery. Thus, the results indicate that loading of BE on the Fe_3O_4 nanoparticles helped in alleviating the EAE severity and progression. Our results are in line with previous reports, stating that berberine, the key antioxidant phytochemical of *Berberis vulgaris*, significantly decreased the severity of clinical symptoms including the loss of tail tonicity, flaccid tail, ataxia and/or paresis and complete paralysis of hind limbs, as well as death in EAE mice (37). As berberine can cross the blood-brain barrier, it can exert beneficial effects on neurodegenerative diseases. Berberine treatment is shown to effectively ameliorate the severity of EAE in C57 BL/6 mice clinically or by neuropathological criteria. It has been previously reported that the medicinal plants possess anti-inflammatory and antioxidant properties, which makes them a natural, safe and reliable remedy for the treatment of neurodegenerative diseases (37).

Previous studies have demonstrated the potential role of NMDARs, being expressed on oligodendrocytes, in demyelination and axonal loss, which are the pathological signs of EAE and MS (38). It is therefore possible that the different efficiency of NMDAR transmission in individuals with different genetic and immune properties can influence other critical aspects of MS pathophysiology. In one study, the effect of barberry juice supplement was determined on the inflammation, caused by intense aerobic activity. This group observed a significant decrease in the expression and function of inflammatory factor, prostaglandin E2 (PGE2) (39, 40).

GRIN1 and GRIN2B mutations and dysfunction, in particular, have been found to be associated with infantile spasms, neurodevelopmental disorders, MS, Alzheimer's Disease, Parkinson's Disease, schizophrenia, obsessive-compulsive disorder, attention/deficit hyperactivity, and bipolar disorder, confirming a

widespread and essential role of NMDARs in brain function and dysfunction. Our qRT-PCR results for the treatment and control group mice-brain mRNA showed a significantly decreased relative expression of *Grin1* in female mice treated with 0.2 and 1 mg of pure BE and a profound decrease in *Grin1* expression was seen in the all Fe_3O_4 + BE groups in a dose-dependent manner. MS is categorized as an autoimmune disorder, in which T cells target the CNS self-antigen in genetically prone individuals (40). NMDA has also been reported to have bipolar properties in MS disease in different sex groups. So, it is necessary to evaluate the separate and coordinated roles of NR1 and NR2 subunits of NMDA ion channel in order to understand the MS progression phenomenon.

CONCLUSION

Grin1 protein is a vital component of NMDA receptor, which plays a key role in the synaptic plasticity and is believed to underlie memory and learning. Our BE-loaded Fe_3O_4 showed a marked decrease in relative expression of *Grin1* gene of NR1 subunit in NMDA ion channel. Our study is the first research on Syrian mice model of EAE and the effect of BE-loaded magnetic nanoparticles on *Grin1* expression in MS model of mice species. It can be concluded from this study that the antioxidant properties of herbal extracts can help to alleviate MS symptoms with fewest side effects.

ACKNOWLEDGMENTS

The authors gratefully acknowledge the support of Research and Technology Foundation of Science and Arts University, Yazd, Iran.

Funding

This research did not receive any specific grant from funding agencies in the public, commercial, or not-for-profit sectors.

Authors' contributions

Experimental layout and EAE mice model generation, experiment supervision and manuscript drafting were done by Amaneh Javid. Main investigator was Fatemeh Noruzifard, and Seyed Mohsen Miresmaili was the adviser, responsible for the gene expression analysis layout and supervision.

CONFLICT OF INTERESTS

The authors declare no conflict of interest.

References

1. Acobucci I, Wen J, Meggendorfer M. Genomic subtyping and therapeutic targeting of acute erythroleukemia. Nat Genet. 2019; 51: 694–704.

2. Hasam-Henderson LA, Gotti GC, Mishto M. NMDA-receptor inhibition and oxidative stress during hippocampal maturation differentially alter parvalbumin expression and gamma-band activity. Sci Rep. 2018; 8: 9545.

3. Franchini L, Stanic J, Ponzoni L. Linking NMDA receptor synaptic retention to synaptic plasticity and cognition. iScience 2019; 19: 927-939.

4. Wyllie DJ, Livesey MR, Hardingham GE. Influence of GluN2 subunit identity on NMDA receptor function. Neuropharmacol. 2013; 74: 4–17.

5. Wyllie DJA. Modelling the details: integrating structure with function. J Physiol. 2018; 596(17): 3833–3834.

6. Malenka R. Intercellular communication in the nervous system. Saint Louis: Elsevier Science, 2014.

7. Dwyer TM. Fundamental neuroscience for basic and clinical applications (Fifth Edition). 2018, Pages 54-71.e1.

8. Lüscher C, Malenka RC. NMDA receptor-dependent long-term potentiation and long-term depression (LTP/LTD). Cold Spring Harb Perspect Biol. 2012; 4(6): a005710.

9. Kim SY, Ahn BH, Kim J, Bae YS, Kwak JY, Min G, Kwon TK, Chang JS, Lee YH, Yoon SH, Min DS. Phospholipase C, protein kinase C, Ca2+/calmodulin-dependent protein kinase II, and redox state are involved in epigallocatechin gallate-induced phospholipase D activation in human astroglioma cells. Eur J Biochem. 2004; 271: 3470-80.

10. Blanke ML, VanDongen AMJ. Activation mechanisms of the NMDA receptor. In: Van Dongen AM, editor. Biology of the NMDA Receptor. Boca Raton (FL): CRC Press/Taylor & Francis; 2009. Chapter 13.

11. Imanshahidi M, Hosseinzadeh H. Pharmacological and therapeutic effects of Berberis vulgaris and its active constituent, berberine. Phytother Res. 2008; 22: 999–1012.

12. Belwal T, Bisht A, Devkota HP, Ullah H, Khan H, Pandey A, Bhatt ID, Echeverría J. Phytopharmacology and clinical updates of Berberis species against diabetes and other metabolic diseases. Front Pharmacol. 11: 41.

13. Rad SZK, Rameshrad M, Hosseinzadeh H. Toxicology effects of Berberis vulgaris (barberry) and its active constituent, berberine: a review. Iran J Basic Med Sci. 2017; 20(5): 516-529.

14. Mirhadi E, Rezaee M, Malaekeh-Nikouei B. Nano strategies for berberine delivery, a natural alkaloid of Berberis. Biomed Pharmacotherapy, 2018; 104: 465–473.

15. Dulińska-Litewka J, Łazarczyk A, Hałubiec P, Szafrański O, Karnas K, Karewicz A. Superparamagnetic iron oxide nanoparticles-current and prospective medical applications. Materials (Basel) 2019; 12: 617.

16. Sankhalkar S, Vernekar V. Quantitative and qualitative analysis of phenolic and flavonoid content in Moringa oleifera Lam and Ocimum tenuiflorum L. Pharmacognosy Res. 2016; 8(1): 16-21.

17. Teng H, Choi O. Optimum extraction of bioactive alkaloid compounds from Rhizome coptidis (Coptis chinensis Franch.) using response surface methodology. Solvent Extr Res Dev 2013; 20: 91–104.

18. Attarde D, Patil M, Chaudhari B, Pal S. Estimation of tannin content in some marketed Harde churna (Terminalia chebula Retz. Family Combretaceae). Int J Pharm Technol 2010; 2(3): 750-756.

19. Gulfraz M, Asad M, Qaddir G, Mehmood S, Shaukat S, Parveen Z. Phytochemical constituents of Berberis lycium royle and Justicia adhatoda. J Chem Soc Pak 2008; 30: 453-457.

20. Singleton VL, Orthofer R, Lamuela-Raventós RM. Analysis of total phenols and other oxidation substrates and antioxidants by means of folin-ciocalteu reagent Author links

open overlay panel. Met Enzymol 1999; 299: 152–178.

21. Karimkhani MM, Salarbashi D, Sanjari Sefidy S, Mohammadzadeh A. Effect of extraction solvents on lipid peroxidation, antioxidant, antibacterial and antifungal activities of Berberis orthobotrys Bienerat ex CK Schneider. J Food Meas Charact 2019; 13: 357–367.

22. Abd El-Wahab AE, Ghareeb DA, Sarhan EE. In vitro biological assessment of berberis vulgaris and its active constituent, berberine: antioxidants, anti-acetylcholinesterase, anti-diabetic and anticancer effects. BMC Complement Altern Med 2013; 13: 218.

23. Rufai Y. Comparative Phyto-constituents analysis from the root bark and root core extractives of cassia ferruginea (Schrad D. C) plant. Scholars J Agri Vet Sci 2016; 3: 275-283.

24. Javid A, Ahmadian S, Saboury AA, Kalantar SM, Rezaei-Zarchi S. Novel biodegradable heparin-coated nanocomposite system for targeted drug delivery. RSC Adv. 2014; 4: 13719-13728.

25. Costanza M. Type 2 inflammatory responses in autoimmune demyelination of the central nervous system: recent advances. J Immunol Res. 2019; 2019: 1-10.

26. Bittner S, Afzali AM, Wiendl H, Meuth SG. Myelin oligodendrocyte glycoprotein (MOG35-55) induced experimental autoimmune encephalomyelitis (EAE) in C57BL/6 mice. J Vis Exp 2014; 86: e51275.

27. (Glatigny S and Bettelli E. Experimental autoimmune encephalomyelitis (EAE) as animal models of Multiple Sclerosis (MS). Cold Spring Harbor Perspectives in Medicine 2018; a028977.

28. Shahi SK, Freedman SN, Dahl RA. Scoring disease in an animal model of multiple sclerosis using a novel infrared-based automated activity-monitoring system. Sci Rep 2019; 9: 19194.

29. Debiyi OO, Sofowora FA. Pytochemical screening of medical plants. Iloyidia. 1978; 3: 234–246.

30. Ahlgren C, Odén A, Lycke J. High nationwide prevalence of multiple

sclerosis in Sweden. Mult Scler. 2011; 17(8): 901-908.

31. Wiedrick J, Meza-Romero R, Gerstner G, Seifert H, Chaudhary P, Headrick A, Kent G, Maestas A, Offner H. Sex differences in EAE reveal common and distinct cellular and molecular components. Cell Immunol 2021; 359: 104242.

32. Zarshenas MM, Ansari R, Dadbakhsh A Mohammadi M. A review of herbal remedies for Multiple Sclerosis-like disorders in Traditional Persian Medicine (TPM)", Curr Drug Metabol 2018; 19(5): 392-407.

33. Wang Y, Liu Y, Du X, Ma H, Yao J. The anti-cancer mechanisms of berberine: A review. Cancer Manag Res. 2020; 12: 695-702.

34. Cardozo C, Inada A, Marcelino G, Figueiredo P, Arakaki D, Hiane P. Therapeutic potential of brazilian cerrado campomanesia species on metabolic dysfunctions. Mol. 2018; 23: 2336.

35. Shirwaikar A, Shirwaikar A, Rajendran K, Punitha ISR. In vitro antioxidant studies on the benzyl tetra isoquinoline alkaloid berberine. Biol Pharm Bull. 2006; 29: 1906–1910.

36. Rossi S, Studer V, Moscatelli A. Opposite roles of NMDA receptors in relapsing and primary progressive multiple sclerosis. PLoS One. 2013; 8(6): e67357.

37. Sharifi-Rad M, Lankatillake C, Dias DA, Docea AO, Mahomoodally MF, Lobine D, Chazot PL, Kurt B, Tumer TB, Moreira AC, Sharopov F, Martorell M, Martins N, Cho WC, Calina D and Sharifi-Rad J. Impact of natural compounds on neurodegenerative disorders: From preclinical to pharmacotherapeutics. J Clin Med 2020; 9: 1061-1079.

38. Ehteshamfar SM, Akhbari M, Afshari JT. Anti-inflammatory and immune-modulatory impacts of berberine on activation of autoreactive T cells in autoimmune inflammation. J Cell Mol Med 2020; 24(23): 13573-13588.

39. Hooshmand Moghadam B, Kordi MR, Mahdian S. The effect of barberry juice supplement on prostaglandin E2 level caused by intense aerobic activity

in active young girls. J Birjand Univ Med Sci. 2017; 24: 1-9.

40. Moradi SZ, Momtaz S, Bayrami Z, Farzaei MH, Abdollahi M. Nanoformulations of herbal extracts in treatment of neurodegenerative disorders. Front Bioeng Biotechnol. 2020; 8: 238.